Stratigraphic Setting, Facies Types, and Mineral Paragenesis of the Carbonate-Bearing Tertiary Sedimentary Succession of Usfan Area, West-Central Saudi Arabia

Ali A. Mesaed
Geo-Exploration Techniques Department, Faculty of Earth Sciences, King Abdulaziz University, Jeddah, Saudi Arabia | Geology Department, Faculty of Sciences, Cairo University, Giza, Egypt
alimesaed@yahoo.com (corresponding author)

Mohamed Gameil
Petroleum Geology and Sedimentology Department, Faculty of Earth Sciences, King Abdulaziz University, Jeddah, Saudi Arabia | Geology Department, Faculty of Sciences, Cairo University, Giza, Egypt
mgameil@yahoo.com

Rayan F. Thiga
Geo-Exploration Techniques Department, Faculty of Earth Sciences, King Abdulaziz University, Jeddah, Saudi Arabia
rthiga@kau.edu.sa

Received: 14 July 2025 | Revised: 29 August 2025 | Accepted: 9 September 2025

 DOI: https://doi.org/10.48084/etasr.13394

ABSTRACT

The present study provides insights into the stratigraphy, facies, and mineral paragenesis of the sedimentary succession of the Usfan area, based on detailed stratigraphic measurements and microscopic descriptions of the different rock units. The study described five distinct rock units: Unit I-Ferruginous sandstone, sandy ironstone; Unit II-Green clays-Phosphatic glauconitic sandstone; Unit III: Fossiliferous Limestone-Dolostone; Unit IV-Green Clay-Glauconitic Ironstone; and Unit V-Tuffaceous Mudstone-Basalt. The depositional environments start with the thinly bedded clastic facies of a lagoonal setting. This is followed by a vertical transition from lagoonal to shallow marine transgression and starved conditions of low clastic input during which the phosphatic green clays were deposited. Subsequently, a period of thick-bedded white fossiliferous limestone succession takes place. After the deposition of the carbonate unit, the area is dominated by a second new marine transgression and deposition of interbedded green clays and glauconitic sandstone. The study also revealed that the area was subjected to progressive regression and subaerial volcanic activities, dominated by the deposition of tuffaceous mudstones under the fluctuation of water depth and the formation of red/green tuffaceous mudstones, overlain by bedded grey tuffaceous basalt, ultimately terminated by black vesicular basalt.

Keywords-Usfan area; tertiary sedimentary succession; green clays

I. INTRODUCTION

The Usfan area is located 100 km NE of Jeddah along Al Haramain Highway, as seen in Figure 1. The measured section is situated to the North of Usan city, about 4 km along the left-hand side of Makkah-Al Madinah Highway. It is characterized by the overturned white carbonate horizon. In the study, the different rock units of the area were identified, laterally correlated, and used to construct a complete stratigraphic section.

A. Background

The geology of Makkah, as depicted in Figures 2 and 3, has been the subject of many studies [1-3]. The Usfan area is located in the northern part of the Makkah district and comprises four main geologic units: the Arabian Shield rocks, the Tertiary sedimentary succession, the Tertiary volcanics

(harrat), and the Quaternary wadi deposits. The Arabian Shield rocks include two main types: 1) intrusive igneous rocks of gabbro, diorite, granodiorite, and granite, 2) layered volcano-sedimentary rocks, either metamorphosed or non-metamorphosed rocks, with Zebarah Samaran and Fatima Groups.

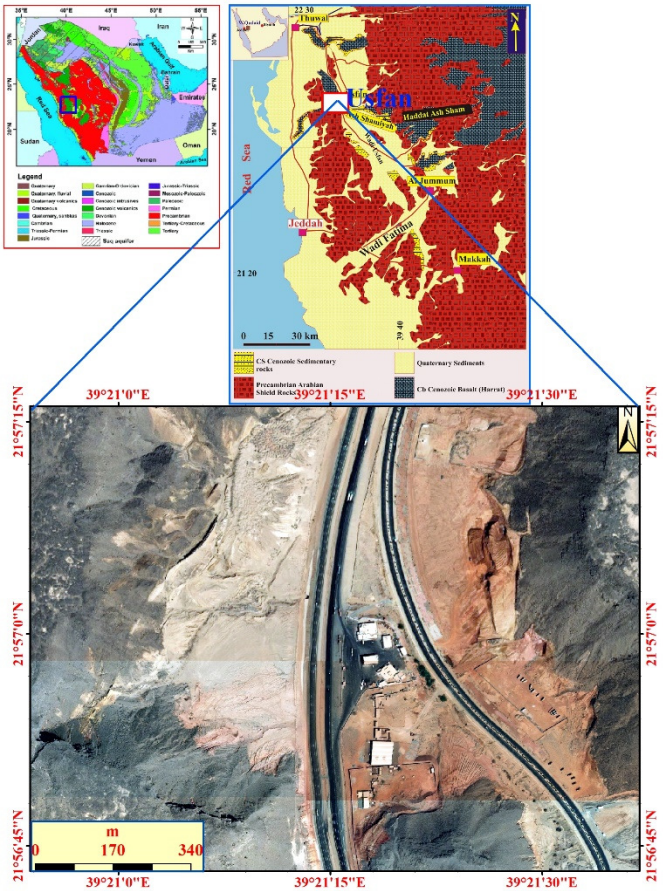

Fig. 1. Detailed geologic maps and satellite image of the study area.

The Tertiary sedimentary succession of the western part of Saudi Arabia was studied in [1, 5, 6]. Most of these studies are focused on the age of this succession, utilizing the paleontological and palynological evidence to determine the accurate succession age. Usfan and Haddat Ash Sham formations and their distribution show that there is a great similarity in the biostratigraphical aspects of Usfan and Haddat Ash Sham formations, where fossils exist in a carbonate unit sandwiched between clastic strata of greater thickness. The molluscan species are similar in both areas, but they are more common in the Usfan than in the Haddat Ash Sham area. They also pointed out that the occurrence of the rudistid Eoradiolites liratus and the nautiloid cephalopod Angulithes mermeti, which are common in the Cenomanian-Turonian strata of North Africa, supports a Cenomanian-Turonian age for the Usfan and Haddat Ash Sham formations.

The succession is underlain by different rock units of the Arabian Shield rocks, and it is also overlain by different facies of the Tertiary volcanics. It is mainly localized along the main NW and NE fault line (Grabens). The geology of the Makkah area, including Usfan, was also studied in [4].

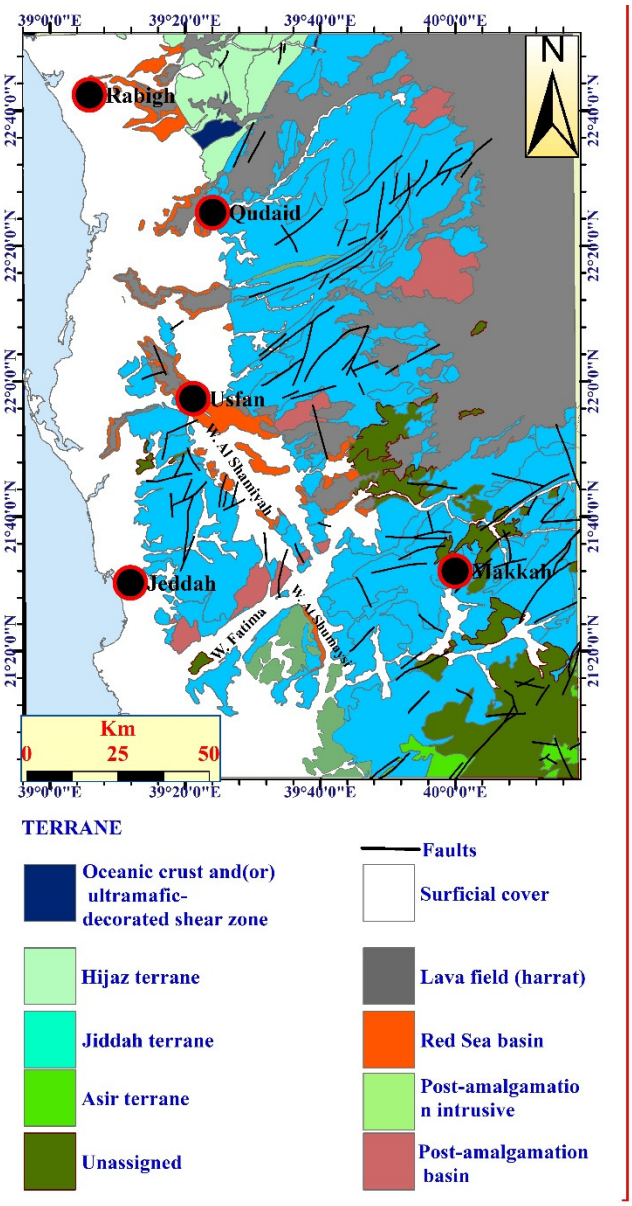

Fig. 2. Geological map of the Makkah district [3].

The carbonates of the studied succession were assigned to the Usfan Formation, which lies conformably on the Haddat Al-Sham Formation and is characterized by its carbonate ledge. According to [7], the formation has been subdivided into three members: lower, middle, and upper. The lower member consists of shale, mudstone, marlstone, sandstone, limestone, and dolomite. The middle member consists of very fine-to-fine quartz sandstone, and the upper part consists of conglomerate layers. The upper member comprises remarkably finer sediments composed of fine-grained sandstone, siltstone, and shale.

Fig. 3. The exposed sedimentary succession of the Usfan area.

The Usfan formation was previously studied in [4, 8, 9]. It is a rift-related sedimentary succession exposed in the western part of Saudi Arabia, particularly near the town of Usfan, North of Jeddah. It forms part of the Phanerozoic sedimentary cover that unconformably overlies the Arabian Shield rocks in the West-central part of Saudi Arabia. The formation was first described during the regional geological mapping campaigns conducted by the USGS in collaboration with the Directorate General of Mineral Resources (DGMR) in the 1960s and 1970s [10, 11]. These studies established that the Usfan Formation consists predominantly of medium- to coarse-grained sandstones, siltstones, and conglomerates, with occasional volcaniclastic interbeds. The report in [12] and the subsequent internal reports by the Saudi Geological Survey (SGS) expanded on these early observations, documenting significant lateral facies variations and thickness changes.

According to [3], the geologic map of the Makkah district, as portrayed in Figure 2, shows the presence of unassigned Arabian Shield rocks in the southeastern corner, with small occurrences of rocks of the Asir terrane. The area is occupied by igneous and metamorphic rocks of the Jeddah terrane, including Hijaze terrane rocks, which are found in the extreme northern part. Ultramafic rocks are only recorded in the North Rabigh area (Jabal Tharwah area). The post-amalgamation intrusive igneous rocks in the area North of Wadi Fatima are represented mainly by granites and diorites. The Red Sea basin rocks (rift-related Tertiary sedimentary succession of the western part of Saudi Arabia) are mainly present along NW wadies (Wadi Al Shumaysi, Wadi Daf, and Wadi Al Shamiyah) and around the Usfan area. Lava field harrat, consisting of Tertiary basic volcanics of the western part of Saudi Arabia, is present in the eastern and northeastern parts of the study area. The Quaternary wadi deposits are present within the major wadies of the Makkah district, including Wadi Fatima, Wadi Al Shumaysi, and Wadi Al Shamiyah.

The present study aims to shed light on the stratigraphic and petrographic data of the carbonate-bearing succession of the Usfan area. In this study, the mineral paragenesis of succession is deduced. The thin carbonates of this succession are very important, and are used for the correlation and dating of the rift-related sedimentary succession of the western part of Saudi Arabia.

II. METHODOLOGY

The study is based on detailed fieldwork, measuring a complete stratigraphic section in the sedimentary succession of the Usfan area. The measured succession is subdivided into five main units. The latter are systematically sampled. The collected samples are used in the preparation of thin sections. Petrographic description of the different units and facies of the measured section is performed to deduce the microfacies and depositional environments. The syn- and post-sedimentary processes and the sequential formation of the different mineral phases (paragenesis) are also achieved in the present study.

III. RESULTS

In this study, a complete stratigraphic section of the exposed part of the Usfan Formation, North of Usfan, as illustrated in Figure 3, was measured. The measured section, as observed in Figure 4, shows the presence of five main units, which are further subdivided. The description of these five units is:

A. Unit I: Ferruginous Sandstone-Sandy Ironstone

1) Description

This unit is up to 40 m thick, as evidenced in Figure 1 and Figure 4 column A. It consists of small-scale cycles of yellow color siltstone, ferruginous sandstones, and is terminated with reddish brown to black sandy and silty ironstones. It is composed of two main large cycles, as seen in column A in Figure 4, and Figures 5(a) and 5(b). The lower cycle, from 0 to 15 m in column A, begins with thick grey mudstone and terminates with sheeted ferruginous sandstone and sandy ironstone beds with thin ferruginous mudstone interbeds, as depicted in Figures 5(c) and 5(d). The second large cycle begins with a green clay horizon, which grades upward into thinly bedded ferruginous fine-grained sandstone with thin mudstone intercalations terminated by egg yellow dolomitic mudstone/dolostone bed, as seen in Figures 4 and 5(e). The microscopic description of this unit led to the recognition of the following petrographic types:

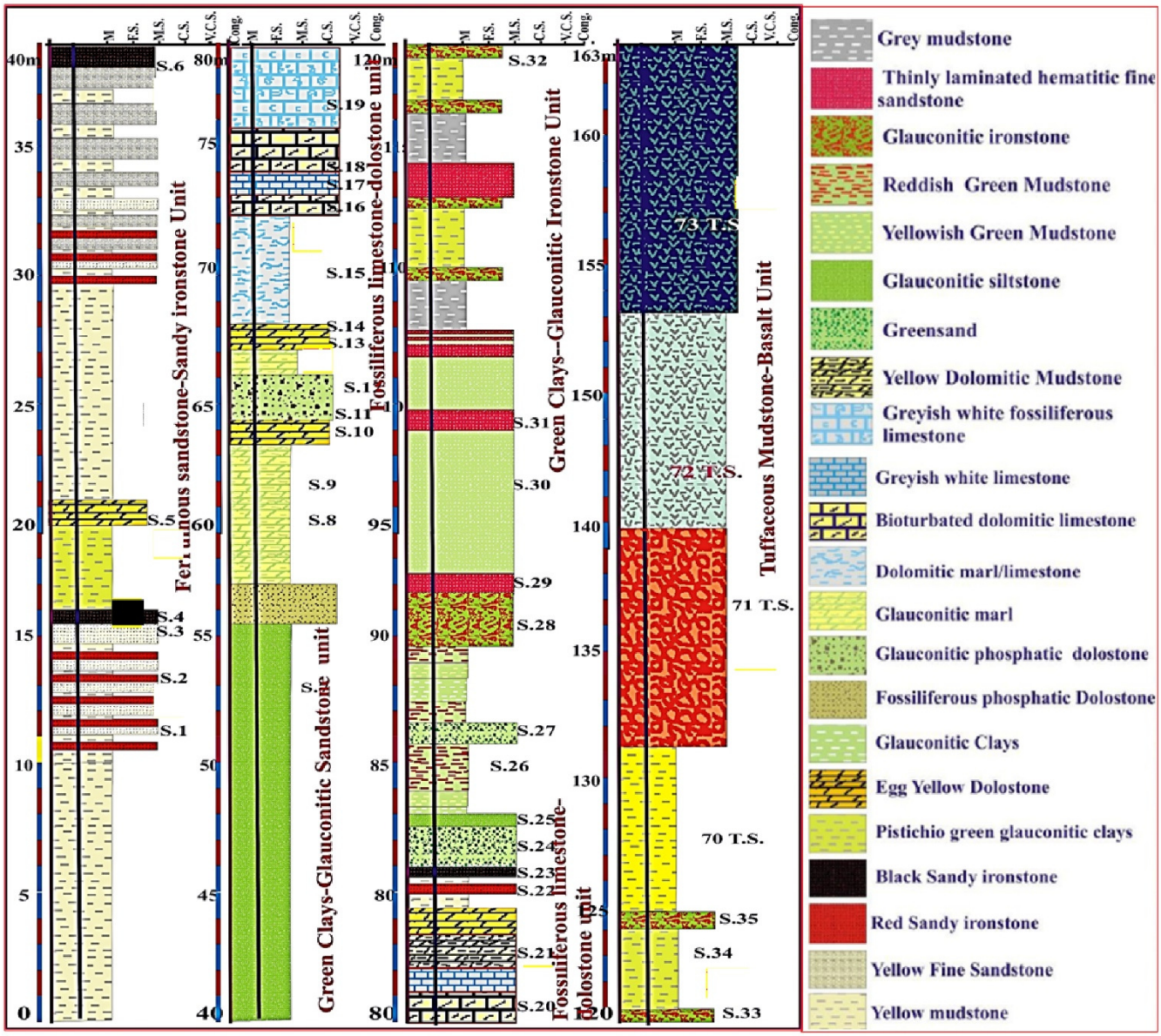

Fig. 4. Complete stratigraphic succession of the Usfan area.

- Kaolinitic-Hematitic fine-grained sandstone T1, which is composed of angular to subrounded, moderately sorted quartz grains embedded within hematitic-kaolinitic matrix/cement. This type grades from grain-supported to matrix-supported domains.
- The matrix-supported domains contain coagulation of amorphous clays mixed with iron oxyhydroxides.
- Hematitic Fine Sandstone T2, as displayed in Figure 6(a), similar to T1 (Figures 6(b-d).
- Kaolinitic-Hematitic Sandstone T3, which is a petrographic lithotype composed of angular to subrounded quartz grains embedded in hematitic cement. The interstitial matrix between the quartz grains is composed of iron-bearing clays (Figures 6(e) and (f)).
- Ferruginous Sandstone-Sandy ironstone T4, as portrayed in Figures 7(a) and (b), is a petrographic lithotype also present in the red sandy ironstone beds of this unit. It consists mainly of angular, moderate to well-sorted quartz grains embedded in black hematitic cement. The quartz grains are found to be highly corroded and embayed by the enclosing hematite cement. Small relics of iron-bearing clays are still present within the interstitial spaces between the quartz grains.
- Yellow dolomitic mudstone-dolostone T5 (Figures 8(c-e) is recorded in the uppermost part of this unit (column A, Figure 4, and Figure 7(c)). It consists of silty calcitized and hematitized iron-rich dolomite, as exhibited in Figures 7(d) and (e).

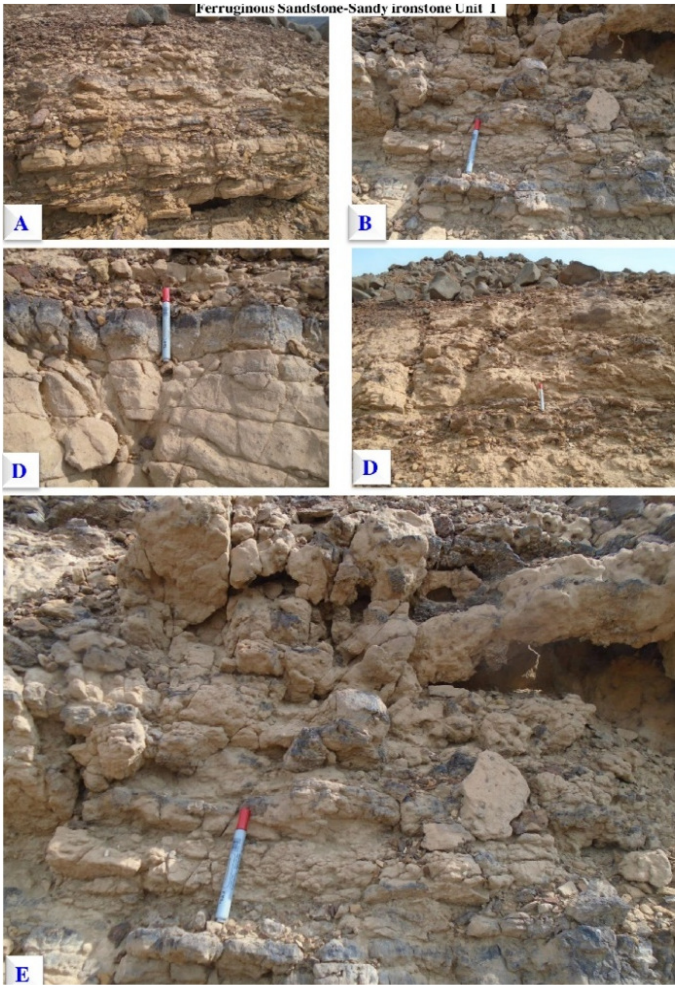

Fig. 5. Unit I: Ferruginous sandstone-sandy ironstone: (a, b) small-scale cycles of yellow color siltstone, ferruginous sandstones, and terminated with reddish brown to black sandy and silty ironstones; (c, d) sheeted ferruginous sandstone and sandy ironstone beds with thin ferruginous mudstone interbeds; and (e) green clay horizon terminated by egg yellow dolomitic mudstone/dolostone bed.

2) Depositional Environments

The presence of horizontal bedded mudstone and ferruginous sandstones indicates deposition in small lakes of a fluctuating water table. The occurrence of green clays, along with the coarsening and thickening-upward nature of this unit, suggests the progressive shallowing of these lakes. This facie is generally laminated, which indicates the deposition of shallow, slight fluctuation in the water depth. The presence of interbedded fine-grained sandstone, siltstone, and mudstone with occasional ripple laminations, flaser bedding, and sparse bioturbation reflects deposition in a shallow, semi-restricted coastal lagoon, where the fluctuating salinity and sediment influx were controlled by the tidal activity or episodic river input.

B. Unit II: Green Clays-Phosphatic Glauconitic Sandstone

1) Description

This unit is present just below the cliff-forming carbonates of the next unit, as seen in column B, Figure 4, and columns B and C, Figure 8(a). It forms a characterized slope-forming unit covered by the limestone boulders of the overlying fossiliferous limestone dolostone Unit III, as shown in Figure 8(a). The green clays and the intercalated glauconitic sandstones are slightly oxidized, resulting in a yellow coloration and the formation of ochreous clays (limonite). The glauconitic sandstones are also oxidized into reddish brown zones, as displayed in Figure 8(a). The microscopic description of this unit led to the recognition of the following petrographic lithotypes:

- Glauconitic sandstone, present in the lower part of the measured stratigraphic section, as illustrated in Figure 4. It consists of an equi-proportion of silt-sized quartz grains and green color glauconite peloids, as demonstrated in Figures 8(b) and (c). These components are embedded within the glauconitic clay matrix, as evidenced in Figures 8(b) and (c). Some of the glauconite peloids and the glauconitic clay matrix become slightly oxidized and get a brownish green color.

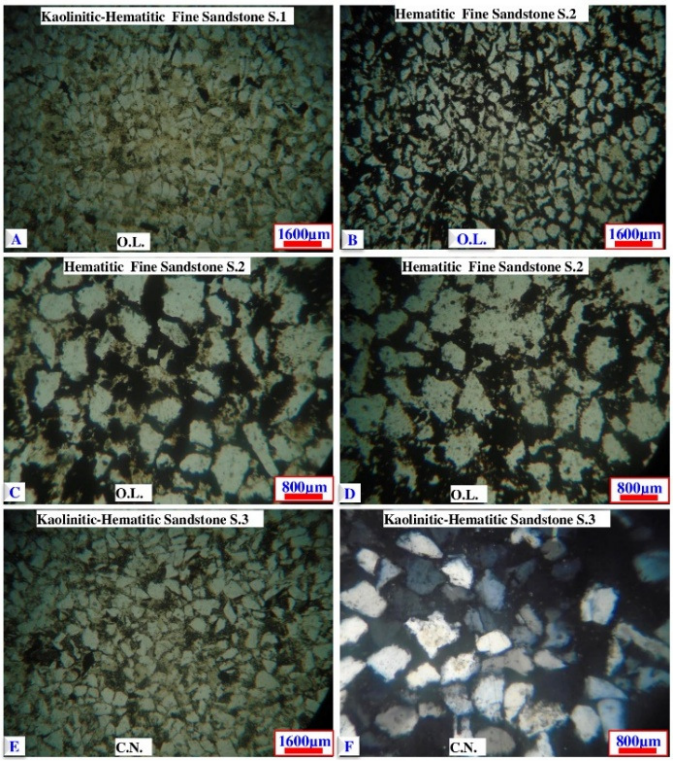

Fig. 6. (a) Kaolinitic-Hematitic fine-grained sandstone T1; (b, c, and d) Hematitic Fine Sandstone T2, similar to T1; (e) and (f) Kaolinitic-Hematitic Sandstone T3 (O.L. Ordinary Light; C. N. Crossed Nicols).

- The fossiliferous calcareous glauconitic sandstone, present in the upper part of this unit, consists of thin limestone interbedded with glauconitic marl, as presented in Figures 8(a) and (b). Microscopically, it consists of fresh (green) and hematitized glauconite peloids (black), and quartz grains within calcite cement, as shown in Figure 8(e). Some large black hematitic domains are formed by the coalescence of black hematite peloids post glauconite peloids. Completely calcitized large shell fragments are

observed to be admixed with the black hematite peloids, as depicted in Figure 8(e). Also, calcite cement becomes highly recrystallized in some domains, giving rise to block calcite crystals of high interference color, as exhibited in Figure 8(e).

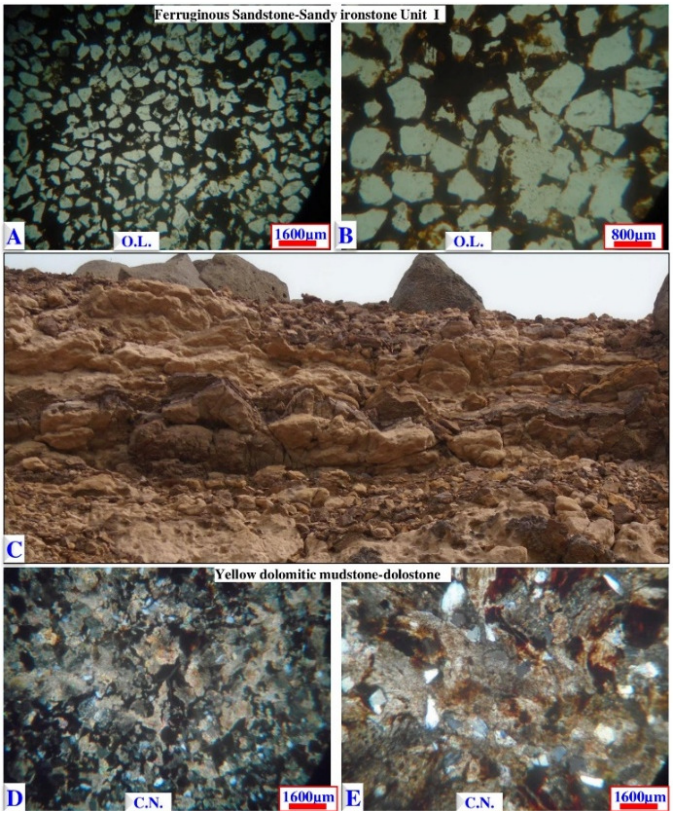

Fig. 7. (a, b) Ferruginous Sandstone-Sandy ironstone T4. (c, d, and e); Yellow dolomitic mudstone-dolostone T5.

- Hematitized phosphatic greensand / glauconitic sandstone, composed mainly of green glauconite peloids, yellow phosphatic peloids, and intraclasts, as presented in Figures 9(a) and (b). These components are cemented by calcite. Most of the glauconite peloids are slightly oxidized, giving rise to blood red (goethite) and black (hematite) patches and domains (Figures 9(a) and (b)). Some slightly oxidized yellowish-green glauconite peloids are still observed within the different components of this petrographic lithotype. Large yellowish-brown amorphous phosphatic intraclasts are also present within this lithotype (Figures 9(a) and (b)). These phosphatic components are also diagenetically recrystallized. Towards the upper parts of the unit, this petrographic lithotype is mainly made up of quartz grains, black hematite peloids, and yellow phosphatic intraclasts. The different constituents are cemented by blocky calcite cement, partially corroded and embayed by the calcite cement.
- Fine dolostone is present as thin yellow color dolomitic mudstone intercalations in the upper part of the cliff-forming unit (Figures 9(c) and (d)).

2) Depositional Environments

The green clays-Phosphatic glauconitic sandstone unit is interpreted as having been deposited in a low-energy marine setting along the middle to the outer shelf, likely during a marine transgression, with slow sediment accumulation, periodic winnowing, and authigenic mineral formation under slightly reducing to suboxic conditions.

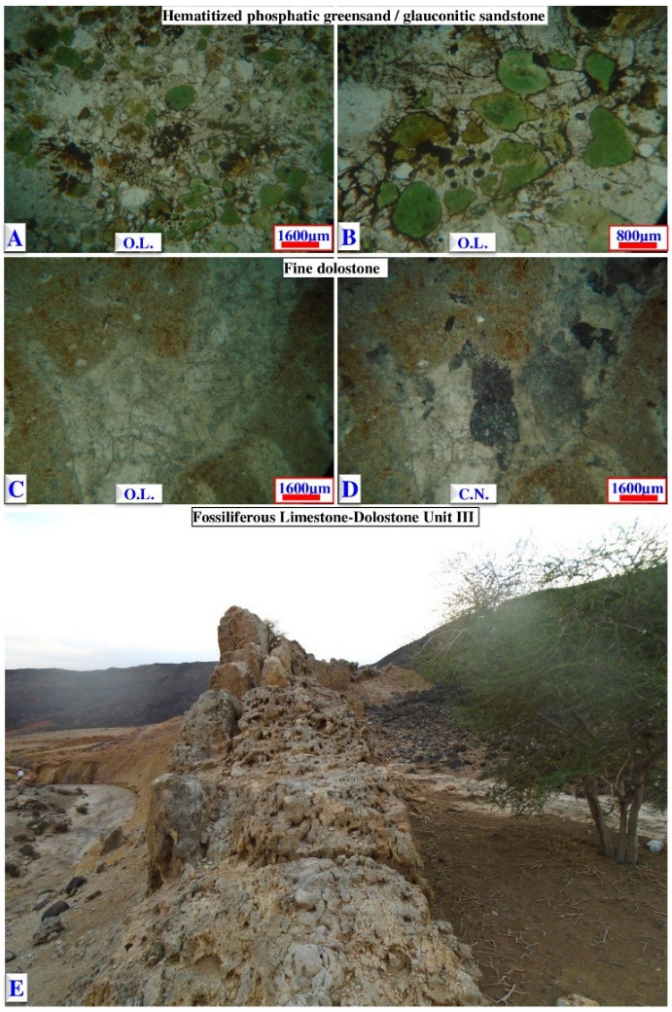

Fig. 8. (a, b) Hematitized phosphatic greensand/glauconitic sandstone; (c, d) fine dolostone; (e) fossiliferous limestone-dolostone of unit III.

The green clays were formed first after the marine transgression during periods of very low clastic input. The presence of phosphatic zones that postdate the green marine clays strongly supports the green clays–phosphorite model (Fe-P pumping theory of formation of marine phosphorites). This model describes how iron (Fe) oxides adsorb phosphate (PO_4^{3-}) in oxic conditions and release it under suboxic to anoxic conditions, contributing to phosphate enrichment near the sediment–water interface and promoting the authigenic phosphorite formation [13, 14]. From the genetic point of view, it is concluded that the marine phosphogenesis processes were carried out just postdate the progressive shoaling, the authigenesis of glaucony facies, and the deposition of Fe and Mg-rich lime-mud in the shallower areas. This authigenesis of

glaucony and the deposition of Ca, Mg-rich lime mud led to the continuous consumption of Al, Si, Fe, Mg, and K from the phosphorite model (Fe-P pumping theory of formation of marine phosphorites). During the progressive and subsequent stages of syn-sedimentary reworking, transportation, and redeposition, phosphorite facies of different mineralogical and chemical characters were deposited. This model is also confirmed in [15, 21, 22].

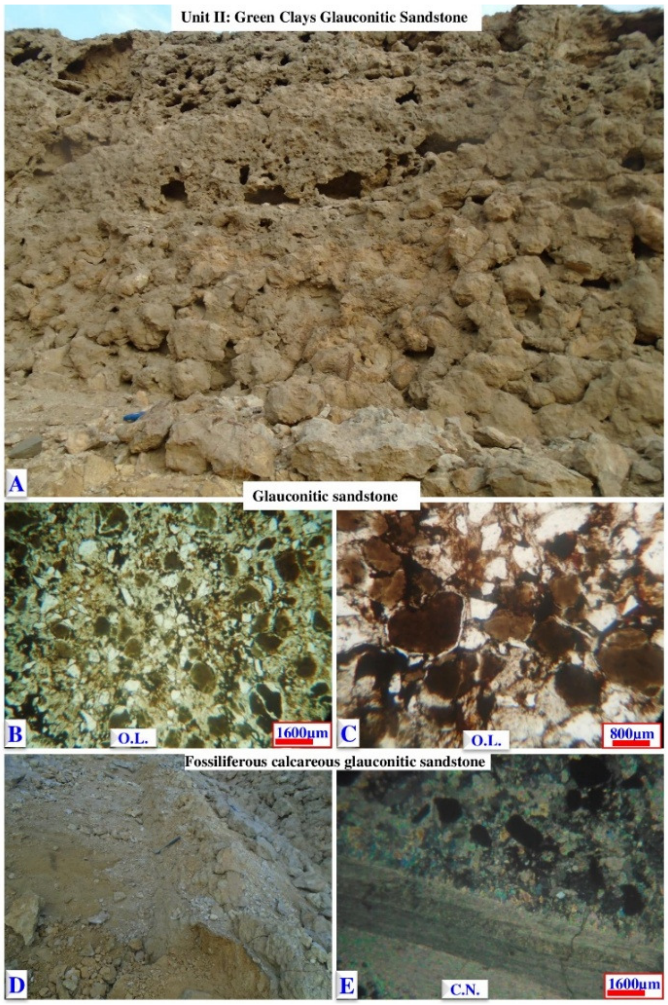

Fig. 9. Unit II: Green clays-Phosphatic glauconitic: (a) characteristic slope-forming unit of green clays and the intercalated glauconitic sandstones; (b, c) glauconitic sandstone; (d) fossiliferous calcareous glauconitic sandstone; and (e) = fresh (green) and hematitized glauconite peloids (black), and quartz grains within calcite cement.

C. Unit III: Fossiliferous Limestone-Dolostone

1) Description

This unit is up to 19 m thick, as seen in column C, Figure 4. It consists mainly of white color cliff-forming, fossiliferous limestone with very thin yellow color dolostone interbeds, as seen in Figure 9(e). The carbonate beds are now present as vertical zones of characteristic pseudo-brecciation nature, as displayed in Figure 10(a). They are enriched with shell and shell fragments of pelecypods and gastropods (Figure 10 (b)). In the lower part of this unit, soft dolomitic marls become enriched with shell fragments and gastropods (Figure 10(b)). The middle part of these units is highly enriched with macrofossils and is present as a vertical ridge of cyclic yellow and grey color carbonates of different lithologic characters and faunal contents. Figure 10(a) shows the close-up view of the interbedded yellow and grey carbonates of the middle part of the unit. The petrographic description of the different horizons of this unit, III, revealed the presence of the following petrographic lithotypes, arranged from base to top as follows:

- Bioclastic grainstone: This petrographic lithotype is present in the middle part of this unit, and it consists of calcitized longitudinal shell fragments embedded with micrite-matrix/ microspar cement (Figures 11(a) and (b)). The micritic matrix exhibits progressive stages of diagenetic recrystallization into microcrystalline calcite. Some non-calcitized dense shell fragments of micritic composition are still seen within the dense micritic matrix. Some of the microspar cement domains become highly recrystallized into coarse crystalline calcite, similar to those formed by the shell fragment recrystallization.

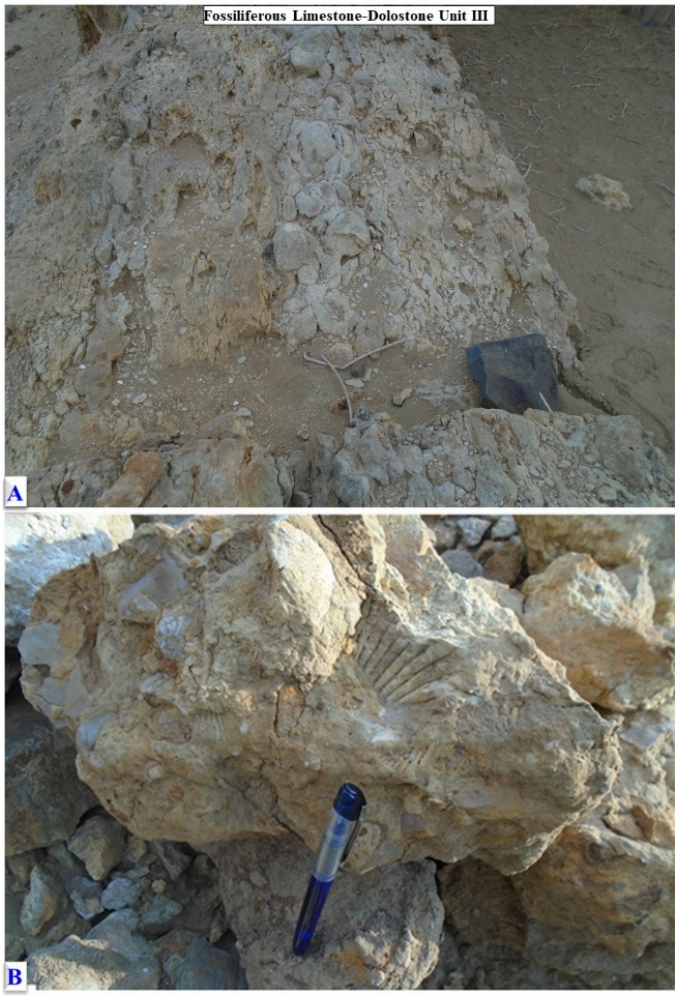

Fig. 10. (a) Fossiliferous limestone-dolostone of unit III; (b) fossiliferous limestone-dolostone enriched with shell and shell fragments of pelecypods and gastropods.

- Calcitized Fe-rich coarse crystalline dolostone: This petrographic lithotype is present just overlying the bioclastic grainstone and consists of coarse crystalline dolomite (iron-rich), containing some calcitized (recrystallized) shell fragments, as depicted in Figure 11(c). The dolomite also shows incipient stages of calcitization and the formation of large domains of blocky calcite. In some of the domains, this petrographic is composed of iron-rich coarse crystalline dolomite. It also demonstrates different stages of ferruginization and calcitization, and the formation of blocky calcite and hematite, and goethite patches and domains (Figure 11(c)).
- Fine crystalline dolostone: This petrographic lithotype is present in the lower part of the unit (Figure 11(d)). It consists of very fine crystalline dolomite/dolomitic mud or dolomicrite. Intensive hematitization and calcitization of the fine iron-rich dolomite are observed along some cracks and veinlets, which have led to the formation of blood red iron oxyhydroxides and blocky calcite.

2) Depositional Environments

Unit III was deposited after the green clays and phosphatic glauconitic sandstone unit. The predominance of bioclastic shell fragments in this microfacies indicates deposition in an agitated condition of an inner shelf environment. The cyclic nature of this unit, as portrayed in Figure 4, argues for the deposition under upward shoaling and the transition from quite deep to shallow subtidal into agitated shallow subtidal-intertidal conditions dominated during the deposition of the uppermost parts of such shallowing-upward cycles. These small cycles also reflect short-lived periods of sea level fluctuation. The predominance of bioclastic debris in the topmost parts of this lithofacies indicates deposition in a highly agitated shallow marine environment [16]. The recognized coarse and fine crystalline dolomites with rare evaporates are in close similarity with the dolostones of the upper intertidal–supratidal zone in platform carbonate that were formed during the sea level fall [17, 18]. The fine crystalline dolomites have been interpreted as a result of penecontemporaneous dolomitization of precursor micrite in supratidal flat sediments during the regressive phase in the upper intertidal to supratidal setting [19]. The presence of bivalve is similar to the microfacies association number 1 [20].

D. Unit IV: Green Clay-Glauconitic Ironstone Unit

1) Description

This unit is present just overlying the carbonate-bearing unit, as observed in column C, Figure 4. It consists of successive small-scale cycles and attains up to 35 m of thickness (Figure 11(e)). Each of these cycles begins with grey thinly laminated mudstone, which grades upward into green glauconitic clays and is terminated by reddish brown to black glauconitic ironstones and ferruginous sandstones, as shown in Figures 12(a) and (b). There is an upward decrease in the thickness and number of the glauconitic ironstone beds from the lower to the upper parts of this unit (Figures 12(a-c)). The microscopic description of this unit led to the identification of the following petrographic lithotypes:

- Hematitized Oxidized greensand: This petrographic lithotype is present as thin reddish brown ironstone beds within the glauconitic clay unit, as illustrated in Figure 12(d). It consists of slightly to completely oxidized glauconitic clay peloids embedded within a slightly hematitized glauconitic clay matrix. The ultimate stages of hematitization have led to the complete hematitization of the green clay peloids and matrix, as portrayed in Figure 12(e).

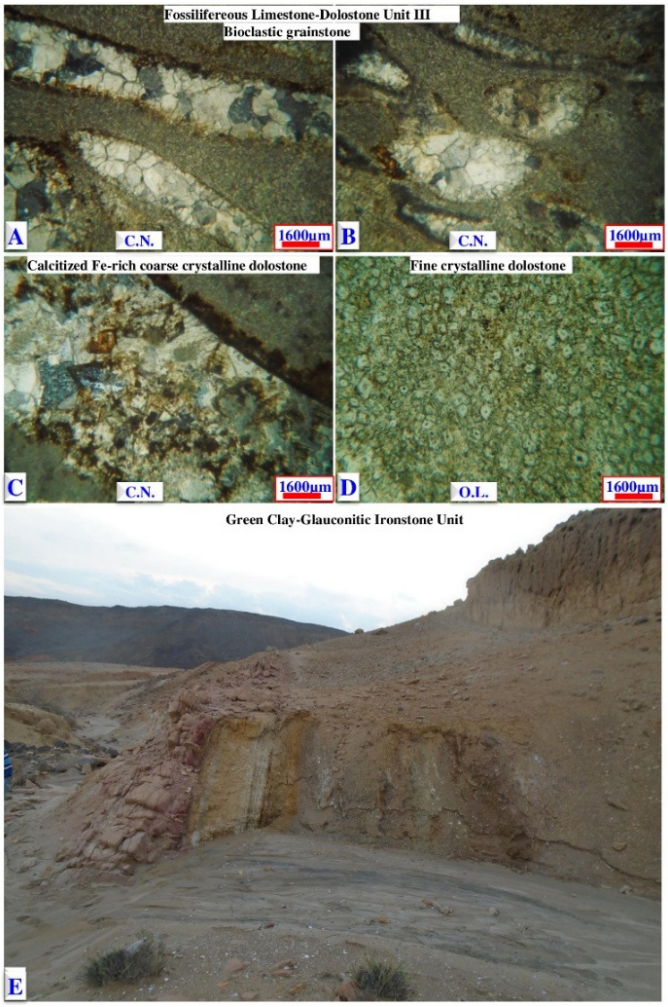

Fig. 11. (a, b) Bioclastic grainstone; (c) calcitized Fe-rich coarse crystalline dolostone; (d) fine crystalline dolostone; (e) unit IV: green clay-glauconitic ironstone unit.

- Hematitic glauconitic sandstone/sandy ironstones: This petrographic lithotype (Figures 12(e-g), is composed of sandy-sized quartz grains admixed with green clay peloids and matrix (Figure 13(f)). The glauconitic clay components become progressively hematitized and turn into a yellowish green color. The ultimate stages of hematitization led to the formation of blood red amorphous iron oxyhydroxides and goethite. The dehydration of these components has led to the formation of black hematite cement. The quartz grains are progressively corroded and embayed by the hematite cement, as presented in Figures 12(g) and (h), leading to the

formation of wide black hematite domains containing very small white quartz relicts, as displayed in Figure 12(f).

2) Depositional Environments

The green clay-glauconitic ironstone unit represents a new transgression, post-dating the restricted conditions that dominated during the upper part of the fossiliferous limestone-dolostone of unit III. The green clays represent deposition in the dysaerobic conditions of high Mg, K, Fe2+, Si4+, and Al3+ cations.

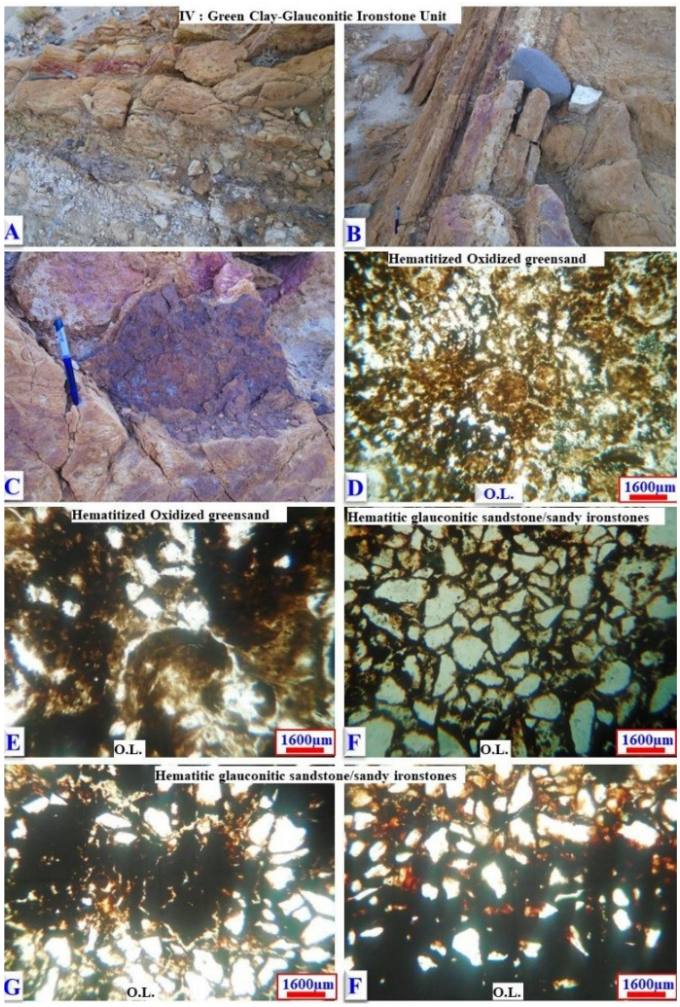

Fig. 12. (a, b) Green clay-glauconitic ironstone unit; (c) glauconitic ironstone beds; (d) hematitized oxidized greensand; (e) ultimate stages of hematitization of the green clay peloids and matrix; (f) hematitic glauconitic sandstone/sandy ironstones; (g, h) blood red amorphous iron oxyhydroxides and goethite.

Their formation is attributed to synsedimentary marine authigenesis (Neoformation theory). The cyclic nature of this unit and the presence of sheet-like glauconitic ironstones in the topmost parts of successive cycles observed in the middle and upper parts of column C, Figure 4, indicate deposition under reducing and oxidizing conditions during the transgressive and regressive cycles. The alternated greensand (unoxidized) zone represents deposition in the reducing dysaerobic conditions of high organic matter content and high ferrous iron activities. This mechanism for the formation of glauconitic ironstone was described in [21] in the Gabal Qalamoon area, Western Desert, Egypt.

E. Unit V: Tuffaceous Mudstone-Basalt Unit

1) Description

This unit is present in the topmost part of the stratigraphic succession, as evidenced in column D, Figure 4 and in Figure 13(a). It consists of four main units, which are arranged from base to top as follows:

- Egg yellow limonitic clays, red sandy slightly oolitic ironstones (Figure 13(b)), grey tuffaceous mudstone Figures 13(a-c)).
- Upper basalt, vesicular and amygdaloidal basalt were found on the topmost part (Figure 13(a)).
- Hematitic tuffaceous sandstone: This petrographic lithotype is composed of isotropic tuffaceous mudstone fragments, quartz grains embedded in tuffaceous matrix (Figure 13(e)). Blood red amorphous iron oxyhydroxides and hematite patches and domains are observed within the interstitial spaces, as shown in Figure 13(f). The hematite patches and domains were formed either through the direct diagenetic hematitization of precursor tuffaceous material or through the hematitization of previously formed green clays.

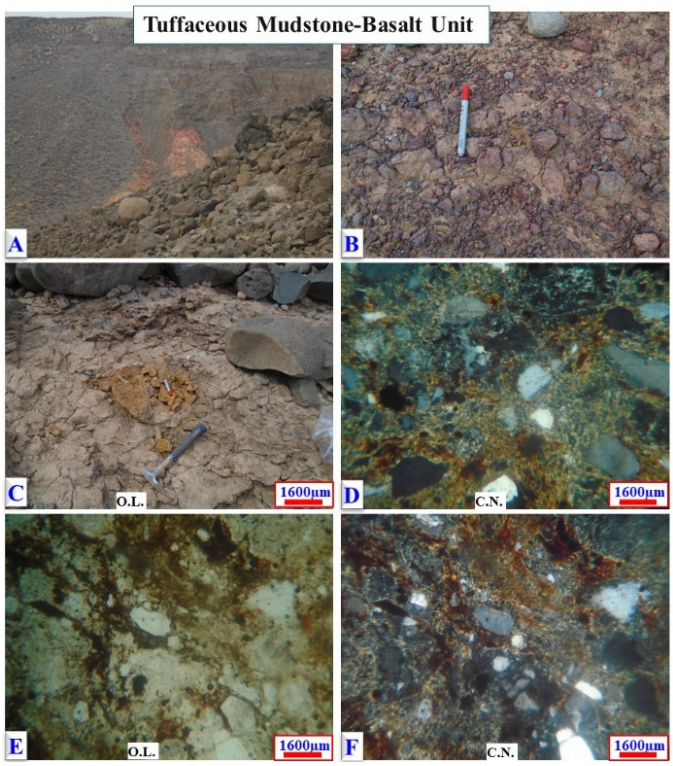

Fig. 13. Unit V: (a) Tuffaceous mudstone-basalt unit; (b) red sandy slightly oolitic ironstones; (c) grey tuffaceous mudstone; (d) upper basalt, vesicular and amygdaloidal basalt on the topmost part; (e) hematitic tuffaceous sandstone; (f) tuffaceous matrix.

2) Depositional Environments

The tuffaceous mudstone-basalt unit V represents subaerial volcanics and related ephemeral lake facies. The volcaniclastic red beds and the overlying tuffaceous glassy basalt and black topmost basalt are equivalent to the Oligocene volcanics and the underlying green and red beds of the North Abu Roash area, Egypt [22]. The tuffaceous mudstone basalt unit is similar to the volcaniclastic red beds of the North Abu Roash area, Egypt [22]. Authors in [22] related the formation of the volcaniclastic red beds into two processes: 1) the direct hematitization of the interstitial precursor tuffaceous materials, which are deposited in shallow oxygenated lagoonal water; 2) the diagenetic oxidation and hematitization of the green clays that were formed under dysaerobic diagenetic conditions.

IV. DISCUSSION

The sedimentary succession in the North Usfan area is of an unexposed base. The equivalent succession in Al Shumaysi and Haddat Asham areas is composed of thick kaolinitic and ferruginous conglomerates and cross cross-bedded sandstone unit of fluviatile environments. The studied succession represents the type locality of the Usfan Formation near Usfan village. The studied succession begins with thinly bedded siltstones of unit I. In other areas around Makkah, the Tertiary sedimentary succession begins with fluviatile conglomerates and sandstones. The coeval succession in the Haddat Asham area was previously studied and subdivided into three main members, representing deposition during earlier continental environments that grade into fluvio-lacustrine and marine, and finally another continental regime at the top.

V. CONCLUSIONS AND DEPOSITIONAL MODEL

In the Usfan area, the succession was deposited during the following stages:

- Stage A: During this stage, the Arabian Shield rocks become exposed and weathered in uplifted source areas, as presented in Figure 14(a). Conglomerates and pebbly sandstone facies were deposited in proximal areas far away from the studied section. Thinly laminated mudstone-sandy ironstone of unit I was deposited, consisting of thinly bedded sandstone/sandy ironstones in successive cycles, and it represents deposition in a lagoonal to fluvio-lacustrine environment. This unit may be equivalent to the fluvio-lacustrine unit II. In the Haddat Asham area, this unit represents deposition in a shoaling lagoon, and it consists of thinly bedded ferruginous sandstone/sandy ironstones in successive cycles. These sandy ironstone units represent deposition in the ultimate stage of shoaling and restriction of the water level.
- Stage B: During this stage, the green clays- glauconitic sandstone of unit II and the overlying fossiliferous limestone -dolostone of unit III were deposited during the marine transgression, as illustrated in Figure 14(b). The formation of green clays/greensand has been described in previous research. The Fe–P pumping theory is supported in this area, as phosphatic glauconitic sandstone occurs in the uppermost part of the green clay succession of this unit, as observed in column B, Figure 4. After a period of green clays-phosphatic greensand, there is a main regression period dominated by the deposition of dolostone and limestones in restricted lagoonal conditions in its lower part. This unit consists of interbedded yellow dolomitic mudstone and dolostone. Above the yellow dolostone unit, the succession consists of cyclic interbedded dolostone and limestone beds that characterize the upper part of this unit. This unit is enriched with large pelecypods and gastropods.

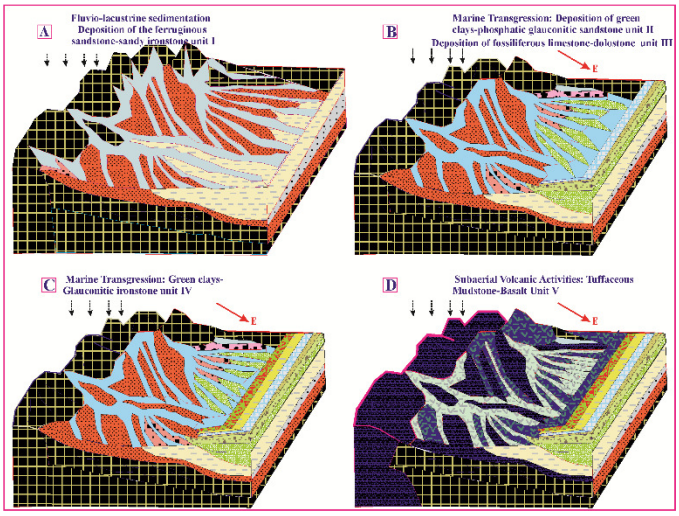

Fig. 14. Stages of the depositional history of the studied succession of the Usfan area.

- Stage C: The time interval (Figure 14(c)) represents a new marine transgression during which the green clays-glauconitic ironstone of unit IV was formed. The green clays represent deposition in dysaerobic conditions of high Mg, K, Fe2+, Si4+, and Al3+ cations. The cyclic nature of this unit, and the presence of sheet-like glauconitic ironstones in the topmost parts of successive cycles, is shown in the middle and upper parts of column C, Figure 4. These glauconitic ironstone beds are the result of the diagenetic oxidation of Fe3+ rich, organic matter, and poor green clays deposited in shallow oxygenated water. Similar glauconitic ironstone is described by in [21] in the Gabal Qalamoon area of the Western Desert in Egypt.
- Stage D: During this time interval, subaerial volcanic activities were dominated by the deposition of basic volcaniclastics in lacustrine depositional sites. The volcaniclastic red beds and the overlying tuffaceous glassy basalt and black topmost basalt are similar to the Oligocene volcanics and the underlying green and red beds of the North Abu Roash area in Egypt. Authors in [22] related the formation of the volcaniclastic red beds to two processes: 1) the direct hematitization of the interstitial precursor tuffaceous materials, which are deposited in shallow oxygenated lagoonal water, and 2) the diagenetic oxidation and hematitization of the green clays that were formed under dysaerobic diagenetic conditions.

REFERENCES

[1] A. M. S. Al-Shanti, *Oolotic Iron Ore Deposits in Wadi Fatima Between Jeddah and Mecca, Saudi Arabia*. Riyadh, Kingdom of Saudi Arabia: Saudi Arabian Directorate General of Mineral Resources, 1966.

[2] T. A. Moore and M. H. Al-Rehaili, "Geologic Map of the Makkah Quaderangle, Sheet 21D," Geologic Map, scale 1: 250,000, Kingdom of Saudi Arabia: Deputy Ministry for Mineral Resources Publication, 1989.

[3] P. R. Johnson, "Explanatory Notes to the Map of Proterozoic Geology of Western Saudi Arabia," Saudi Geological Survey, Jeddah, Kingdom of Saudi Arabia, Technical Report SGS-TR-2006-4, 2006.

[4] M. A. M. Alghamdi and A. Z. E. A. Bishta, "Preliminary Site Investigation based on RGB Electromagnetic Energy of Landsat-7 Images in Wadi Fayidah, Saudi Arabia," *Engineering, Technology & Applied Science Research*, vol. 13, no. 2, pp. 10595–10600, Apr. 2023, https://doi.org/10.48084/etasr.5800.

[5] J. G. Moltzerand and P. L. Binda, *Micropaleontology and Palynology of the Middle and Upper Members of the Shumaysi Formation, Saudi Arabia*. Jeddah, Kingdom of Saudi Arabia: Faculty of Earth Sciences Bulletin 4, King Abdulaziz University, 1983.

[6] F. A. Alqahtani, M. R. Abdulfarraj, and H. A. Wanas, "Depositional Architecture and Sequence Stratigraphic Framework of the Fluvio-lacustrine Ash Shumaysi Formation, Jeddah-makkah Region, Saudi Arabia: Implications for Climatic and Tectonic Changes in a Local-scale Sub-basin," *The Depositional Record*, vol. 9, no. 4, pp. 1066–1094, Nov. 2023, https://doi.org/10.1002/dep2.248.

[7] R. Zeidan and K. Banat, *Petrology, Mineralogy and Geochemistry of the Sedimentary Formations in Usfan, Haddat Ash-sham and Shumaysi Areas, and Their Associated Oolitic Ironstone Interbeds, Northeast and East of Jeddah, Saudi Arabia*. Jeddah, Kingdom of Saudi Arabia: King Abdulaziz University, Directorate of Research Projects, 1989.

[8] J. W. Smith, "Reconnaissance Geologic Map of the Wadi Mahani Quadrangle, Sheet22/40a, Kingdom of Saudi Arabia," Geologic Map GM-35, 1:100,000 Scale, Saudi Arabian Deputy Ministry for Mineral Resources, Jeddah, Kingdom of Saudi Arabia, 1981.

[9] J. W. Smith, "Reconnaissance geologic map of the Wadi Hammah quadrangle, Sheet22/40C," Geologic Map GM-65, 1:100,000 Scale, Saudi Arabian Deputy Ministry for Mineral Resources, Jeddah, Kingdom of Saudi Arabia, 1981.

[10] G. F. Brown, R. O. Jackson, R. G. Bogue, and W. H. MacLean, "Geology of the Southern Hijaz Quadrangle," Geologic Map, 1: 500,000 Scale, Saudi Arabian Directorate General of Mineral Resources, Jeddah, Kingdom of Saudi Arabia, 1963.

[11] R. W. Greenwood, "Geology of the Asfan Quadrangle, Sheet 21/42 A," Geologic Map, 1:100,000 Scale, Saudi Arabian Directorate General of Mineral Resources, Jeddah, Kingdom of Saudi Arabia, 1975.

[12] D. G. Hadley and D. L. Schmidt, "Sedimentary Rocks of the Usfan Area, Western Saudi Arabia," Saudi Arabian Directorate General of Mineral Resources, Jeddah, Kingdom of Saudi Arabia, Technical Report USGS-OF-03-105, 1980.

[13] P. N. Froelich, M. L. Bender, and N. A. Luedtke, "The Redox Chemistry of the Modern and Ancient Sedimentary Iron Cycle," *Earth-Science Reviews*, vol. 19, no. 2, pp. 121–140, Apr. 1983.

[14] G. M. Filippelli, "The Global Phosphorus Cycle: Past, Present, and Future," *Elements*, vol. 4, no. 2, pp. 89–95, Apr. 2008, https://doi.org/10.2113/GSELEMENTS.4.2.89.

[15] C. R. Glenn and M. A. Arthur, "Petrology and Major Element Geochemistry of Peru Margin Phosphorites and Associated Diagenetic Minerals: Authigenesis in Modern Organic-rich Sediments," *Marine Geology*, vol. 80, no. 3–4, pp. 231–267, May 1988, https://doi.org/10.1016/0025-3227(88)90092-8.

[16] A. M. Abdallah, N. M. Abouel Ela, and S. G. Saber, "Lithostratigraphy, Microfacies and Depositional Environments of the Creta- Ceous Rocks at Gabal Halal, Northern Sinai, Egypt," in *3rd International Conference on Geology Arab World*, Cairo, Egypt, 1996, pp. 381–406.

[17] M. A. Khalifa, "Depositional Cycles in Relation to Sea Level Changes, Case Studies From Egypt and Saudi Arabia," *Egyptian Journal of Geology*, vol. 40, no. 1, pp. 141–171, 1996.

[18] M. Abu El-Hassan and H. A. Wanas, "Dolomitization of the Cenomanian–turonian Carbonate Rocks Along the Western Side of the Gulf of Suez: Implication to Sea Level Oscillations," *Bulletin Faculty Science Alexandria University Egypt*, vol. 43, pp. 245–270, 2005.

[19] J. L. Wilson, *Carbonate Facies in Geologic History*, 1st Ed. New York, NY: Springer New York, 1975.

[20] E. Flügel, *Microfacies of Carbonate Rocks: Analysis, Interpretation and Application*. Berlin, Germany: Springer Berlin Heidelberg, 2010.

[21] A. A. Mesaed, "Mechanism of Formation of the Upper Eocene Glauconitic Ironstones and Red Beds of Gabal Qalamoon area, Western Desert, Egypt," *Egyptian Journal of Geology*, vol. 48, pp. 17–44, 2004.

[22] A. A. Mesaed, "Mechanism of Formation of the Oligocene Volcaniclastic Red Beds and the Associated Tephra Deposits, North Abu Roash Area, Egypt," in *7th International Conference on the Geology of the Arab World*, Cairo, Egypt, 2004, pp. 165–182.